International Communications in Heat and Mass Transfer 148 (2023) 107006

Contents lists available at ScienceDirect

International Communications in Heat and Mass Transfer

journal homepage: www.elsevier.com/locate/ichmt

Influence of condenser bypass port area on maximum thermal load of heat pipe

Cheong Hoon Kwon [a], Gee Chan Jin [a], Jun Hyung Kim [a], Bo Gyu Im [a], Ji Hoon Jeong [a], Eui Guk Jung [b,*]

[a] Department of Energy Resources and Chemical Engineering, Kangwon National University, Kangwon-do 25913, Republic of Korea
[b] School of Mechanical System Engineering, Kangwon National University, Kangwon-do 25913, Republic of Korea

ARTICLE INFO

Keywords:
Maximum heat transfer rate
Startup
Heat transfer performance
Bypass mass flow rate
Dryout
Heat pipe
Liquid bypass tube

ABSTRACT

Experimental works have been conducted to enhance the performance of heat pipes by focusing on the maximum thermal load, which is a very important performance indicator. Ordinal operation on the heat pipe occurs when the capillary force is sufficient to overcome the flow resistance of the working fluid. Therefore, one method of increasing the maximum thermal load is to reduce the flow resistance of the liquid and vapor with counter flow in the system. Moreover, the flow resistance of the working fluid is immediately dependent on the mass flow rate, and reducing the flow rate can effectively increase the maximum thermal load. The liquid bypass technique is one method of alleviating the flow resistance of the working fluid inner side a heat pipe container. In this work, a modified heat pipe system with one liquid bypass tube was manufactured and investigated, with the bypass tube being constructed so that some of the working fluid inside the condenser could be bypassed to an evaporator not going through a heat pipe interspace with vapor and liquid counterflow. Three bypass ports were located in the condenser; hence, the influence of bypass port area on thermal of heat pipe performance was investigated experimentally. Mass flow rate control valves were attached to these three bypass ports, and the maximum thermal loads according to the activation of each port were experimentally measured. The maximum thermal load in a horizontal position increased by up to 45.8% with an increase in the area of the bypass port. With the increase of the activated bypass port area, the condenser wall temperature increased by up to 15.9 °C.

1. Introduction

1.1. Literature review

In the design of cutting-edge mechanical components, a common objective is to maximize performance while minimizing size; this objective also applies to the design of thermal management devices. Indeed, heat pipes have attracted attention as the most realistic cooling solutions for highly integrated electronic products, as they require no additional power sources, completely insulate the working fluid and electronic circuits, and can separate the heating and heat dissipation sections by a certain distance.

Recent studies on heat pipes have mainly focused on industrial applications. In particular, the importance of two-phase heat transfer devices in the thermal handling of electric- and hydrogen-vehicle battery systems is increasing [1–4], as the fuel cell stack used as an electric-vehicle power source operates the most effectively within a specific temperature range. In addition, thermal energy in a fuel cell system may be recovered at a high rate using heat pipes, and this possible application is attracting increasing research attention.

A classical heat pipe is comprised of a closed cylindrical container, which mainly contains an evaporator, condenser, and adiabatic section, as indicated in Fig. 1. Previous studies aiming to improve thermal performance of heat pipe have mainly focused on design of capillary wick structure because the heat transfer performance of a heat pipe is mainly dependent on capillary pressure. The capillary pressure, $p_{cap.}$ [$=2\sigma/r_{men.}$] is directly proportional to the working-fluid surface tension and inversely correspondent to the pore radius of the porous capillary wick material; thus, the thermal performance fundamentally is subject to the design of the capillary wick and the selected working fluid [5]. Regarding the capillary structure, when the pore size on the wick structure is decreased, the capillary force that induces the driving power required to circulate the working fluid may increase. However, the thermal performance may be negatively affected by the corresponding increase in the pressure drop of the liquid going back to the evaporator.

* Corresponding author.
E-mail addresses: chkwon2@kangwon.ac.kr (C.H. Kwon), egjung@kangwon.ac.kr (E.G. Jung).

https://doi.org/10.1016/j.icheatmasstransfer.2023.107006

Nomenclature

A	area (m^2)
BOM	bypass-line operation mode
BL	bypass line
c	specific heat (J/kg·°C)
F	friction coefficient
g	acceleration of gravity (m/s^2)
K	hydraulic permeability (m^2)
L	length (m)
$\dot{m}$	mass flow rate (kg/s)
NOM	normal operating mode
p	pressure (pa)
Q	thermal load (W)
r	radius (m)
R	thermal resistance (°C/W)
Re	Reynolds number
T	temperature (°C)
U	uncertainity
u	velocity (m/s)
$\dot{V}$	volumetric flow rate (m^3/s)
z	axial position of heat pipe
Φ	working-fluid fill charge ratio
μ	viscosity (pa·s)
ρ	density (kg/m^3)
φ	heat pipe inclination angle (°)
σ	surface tension (N/m)
τ	sheer stress (pa)

Subscripts

adia.	adiabatic
bl	bypass line
cap.	capillary
cond.	condenser
cool.in	coolant inlet
cool.out	coolant outlet
evap.	evaporator
in	input
l	liquid
loss	loss
max.	maximum value
men.	meniscus
min.dryout	minimum thermal load causing dryout
t	total
th	thermal
v	vapor
w	wick or wall

In general, when the driving force is lower than the summation of the vapor and liquid pressure drops, the dryout phenomenon occurs. In other words, dryout may take place in the wick of the evaporator for all thermal load ranges, causing a pressure drop for the working fluid greater than the head in the capillary pressure. Thus, a critical thermal load exists; this load is generally referred to as the "capillary limit" [5] and governs the maximum heat transfer rate (hereafter referred to Q_{max}).

Previous studies [6–8] on the capillary limit and dryout have provided valuable physical insights into the operating limits of heat pipes and revealed that dryout over the capillary wick structure is caused by insufficient liquid supply to the starting area of the evaporator. Thus, experimental studies visualizing the dryout phenomenon of the capillary structure have provided useful methods of improving heat transfer performance by preventing dryout. According to the previous research results, dryout can be prevented by sufficient liquid supply to the evaporator corresponding to the input thermal load. Return of the liquid can be achieved by capillary pressure in the operation of the heat pipe. Therefore, studies on the improvement of the maximum heat transfer rate resulting from dryout have mainly focused on the design of the capillary structure or the improvement of the physical properties of the working fluid to improve the capillary force. In addition, attempts have been made to improve the maximum thermal load by improving the physical properties of the working fluid.

Regarding the performance enhancement of capillary structures, Brautsch and Kew [6] previously reported experimental results in which the value of Q_{max} that causes dryout was increased by increasing the number of screen mesh layers, where those layers were used to ensure a sufficient liquid region inside the heat pipe. They visually presented the evaporation process in the wick with a screen mesh. In their visualization experiment, the capillary structure was locally dried by internal vapor formation and entrapment, and interruption of the liquid supply over a trapped vapor bubble was observed. Similarly, Kempers et al. [7] experimentally analyzed the influence of the screen mesh number and fill charge ratio on the operating fluid on Q_{max}. In their experiment, an appropriate number of screen mesh layers and a higher fill charge ratio of the working fluid improved the isothermal performance of the heat pipe, because the temperature discrepancy between the walls of the evaporator and condenser was reduced and, hence, Q_{max} was increased.

Wong et al. [8] installed sintered-copper-powder-mesh wicks and homogeneous copper-powder wicks in working flat-plate heat pipes and visually measured and compared the evaporation resistances of these wick structures. In their experiments, the fine powder was found to help liquid return by reducing evaporation resistance and flow resistance. In an experiment performed by Revellin et al. [9], the width of the microgroove in a micro heat pipe was increased. As a result, a sufficient liquid flow path was ensured, dryout was prevented, and the maximum heat flux was increased. However, an excessive raise in the capillary structure area negatively affected the thermal performance by increasing the pressure drop in both the vapor and liquid regions. Moreover, in an experiment conducted by Lefeveré and Lallemand [10], a larger number of screen layers and a thicker sintered porous wick decreased the thermal capacity of micro heat pipes. Wong and Liao [11] fabricated heat pipes having a composite wick composed of a mesh-groove and a non-composite wick; an improved Q_{max} was obtained for the heat pipe in which the composite wick was applied. For a flat heat pipe, the dependency of the container thickness on the thermal performance was experimentally measured by Lips et al. [12]. In their study, a decrease in

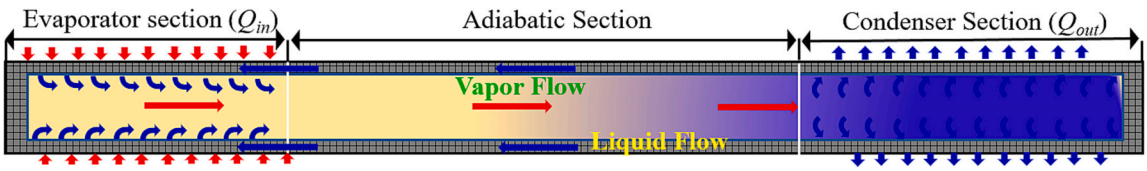

Fig. 1. Schematic diagram of typical heat pipe showing working-fluid circulation.

the thickness of the flat heat pipe caused an increase in the curvature of the evaporation interface. The decrease in capillary pressure due to the increase in curvature resulted in a decrease in the maximum thermal load. Wong et al. [13] also reported experimental results in which Q_{max} was improved when different mesh numbers for the screen capillary structure were favorably combined; this improvement occurred because higher capillary pressure could be achieved.

On the other hand, the maximum thermal loads for various working fluids have been investigated by several researchers. In general, a working fluid is selected based on compatibility with a heat pipe container. With inappropriate compatibility, the heat transfer performance of the heat pipe may be seriously deteriorated by the non-condensable gas produced by the chemical reaction between the working fluid and the container. The maximum thermal loads for water, methanol, and acetone were reported by Wong et al. [13]. Water had the highest maximum thermal load among the considered working fluids. Cecere et al. [14] experimentally defined the relationship between the wettability and dryout of numerous working fluids through a surface treatment in which aluminum nanoparticles were deposited on the inner surface of the heat pipe. In addition, Pruzan et al. [15] experimentally compared the heat capacities of the heat pipes in which the binary mixture determined by a particular mole fraction or a pure water, respectively, were employed; higher dryout heat flux was observed for the binary mixture. These previous studies have mainly focused on the proper combination of capillary structures, optimization of groove configurations, and physical properties of working fluids to improve the maximum thermal loads of heat pipes.

1.2. Background information

Studies have been conducted in which typical heat pipes have undergone structural modifications based on physical investigation of the fluid flow mechanisms within the internal space of the heat pipe. As shown in Fig. 1, flow resistance occurs on the interface of phase change between the vapor and liquid with counter flow inside the heat pipe. This feature leads to a decrease in thermal performance. For example, a typical heat pipe cannot operate normally under a reverse gradient (where the evaporator is above the condenser) due to the flow resistance caused by the counter flow of vapor and liquid. To solve this problem, a loop heat pipe (LHP), which completely separates vapor and liquid to eliminate interface flow resistance, was developed after the 1970s [16]. Although LHPs are known to have strong operating performance and excellent heat transfer performance compared to typical heat pipes, considerable technical difficulties exist in fabricating sintered metal wicks with fine pores or applying them as thermal control devices in mechanical systems. Accordingly, the application to the ground mechanical system is not generalized because the price of an LHP system is very high. Consequently, the development of LHPs has mainly been conducted in advanced aerospace countries for thermal control of space vehicles.

Recently, studies have been conducted to achieve improved heat transfer performance by reducing the interface resistance of the working fluid. Jung and Boo [17] connected the beginning of the evaporator and the end of the condenser with a bypass line. Their research aimed to improve the heat transfer performance by inducing a decrease in the flow resistance of the working fluid within the heat pipe by bypassing a part of the condensed liquid to the beginning of the evaporator by the bypass line without passing through the inside of the heat pipe. In their study, the liquid mass flow within the heat pipe was reduced by the liquid bypass, and consequently, the pressure drop between the vapor and liquid inside the heat pipe can be reduced. Improvement of thermal performance by accelerating the working fluid can be achieved as the pressure drop between the vapor and the liquid inside the heat pipeis reduced by inducing a decrease in the liquid mass flow rate inside the HP by the bypass line. In their study [17], the maximum thermal load was increased by up to 35.5% by applying the bypass line, and the thermal resistance of heat pipe by the bypass line under steady state [18] was reduced by up to 61% by Baek and Jung [18]. Their experimental study revealed for the first time that a decrease in liquid mass flow within a typical heat pipe effectively improves the heat transfer performance. The advantages of the LHP can be obtained very simply by applying a bypass line to a typical heat pipe.

This study was conducted as an extension of the previous works [17,18]. In the previous studies, the effect of liquid bypass on heat pipe thermal performance was investigated in a very simple and conceptual manner. As shown in Figs. 2 and 3(b), full separation of the liquid and vapor by the bypass line is impossible. Only a part of the liquid can be separated from the inner space of the heat pipe. Considering the operating characteristics of the LHP, the larger the amount of the bypassed liquid, the more the flow resistance to the working fluid in the heat pipe internal space is reduced, so the heat transfer performance will be increased further. Therefore, a rational design for the bypass line should be developed so that as much liquid as possible can be bypassed. The dependence between the change in the mass flow rate of the liquid or vapor bypassed or separated from the heat pipe and the heat transfer performance has not been experimentally identified. Moreover, in experimental studies on dryout [19,20], the thermal load that the heat pipe could operate normally without the capillary was limited by the lack of liquid resupplied to the evaporator. Therefore, a thermal load capable of normal operation may be increased as the liquid resupplied to the evaporator by the bypassed liquid may increase. Moreover, the more liquid bypassed, the higher the thermal load that causes dryout can be.

The purpose of this study was to obtain experimentally the effect of an increase in the bypassed mass flow rate on the maximum thermal load of heat pipe. The dependence between the increase in the condenser area open to the bypass pipe and the maximum thermal load that can operate normally without dryout was experimentally presented. This issue has not been dealt with in previous studies [17,18]. In particular, as shown in Figs. 2 and 3(b), three liquid bypass ports were modeled to the condenser to investigate the effect of the mass flow rate of the liquid bypassed from the condenser to the evaporator on the maximum thermal load. The heat pipe system was modified so that the bypassed mass flow rate could be manually controlled according to the number of bypass valves activated. As the amount of liquid bypassed increases, the amount of liquid re-supplied to the evaporator may increase. In addition, the pressure drop for the liquid and vapor in the inner space of the heat pipe is further reduced. With these advantages, the experiments in this study were conducted. The technique of measuring pressure and mass flow rate by using a measuring instrument has not been known until now because a heat pipe is basically operated under saturation conditions. The bypass port area may be defined as the area of the condenser opened to the bypass tube. Therefore, the liquid mass flow rate was assumed to increase with an increase in the number of activated ports, and experiments were performed under four operating modes according to the number of activated bypass ports. Although various techniques for increasing the mass flow rate on the bypassed liquid may exist, enlargement of bypass port area of the condenser may be one useful method.

A study on the technique of increasing the bypass port area of the condenser to bypass more liquid was beyond the scope of this work. Because the focus of this study was on whether the maximum thermal load increases or decreases according to the increase in the mass flow rate of the bypassed liquid, bypass ports were installed at equal intervals at the beginning, middle, and end of the condenser for convenience. In addition, the diameter of the bypass tube was appropriately selected considering the diameter of the heat pipe. As shown in Fig. 2, each port can be activated separately by the bypass valve so that the bypass mass flow rate can be controlled. The maximum thermal load according to the number of bypass ports activated under various operating conditions was experimentally obtained. The mass flow rate of the liquid to be bypassed can be very strongly dependent on the area or location of the bypass tube opening in the condenser. Unfortunately, theoretical models

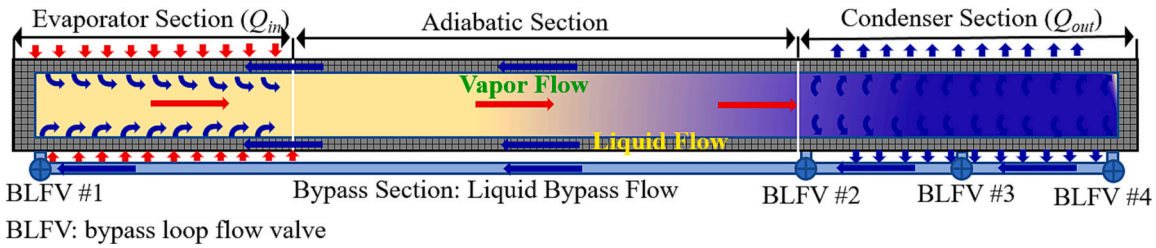

Fig. 2. Schematic diagram showing physical operation of heat pipe with liquid bypass line.

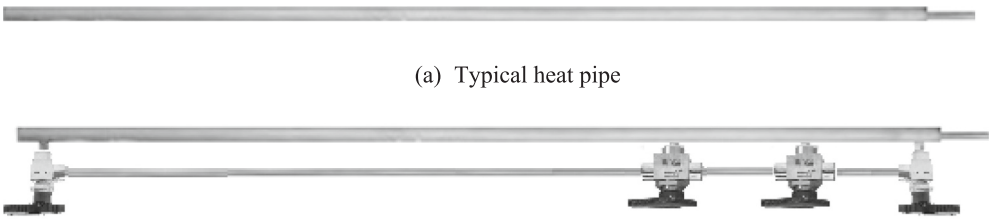

Fig. 3. Photographs of (a) typical heat pipe and (b) heat pipe with bypass line.

capable of effectively designing the bypass flow path are not known, and moreover, an analytical model for the bypassed liquid mass flow rate has not been developed. Therefore, this work is limited to an experimental approach, and a theoretical approach to the heat transfer performance analysis of the heat pipe attached with the bypass line is outside the scope of this study.

2. Experimental setup and procedure

The heat pipe geometry and working fluid used in this work were identical to those in Refs. [17, 18]. Fig. 3(a) is an image of the typical heat pipe employed in this study. Fig. 3(b) shows the examined heat pipe, which had one bypass port in the evaporator and three bypass ports at the start, middle, and end of the condenser. As apparent from Fig. 3(b), the liquid mass flow could be bypassed to the evaporator by the three bypass ports in the condenser. A flow control valve was attached to each bypass port, so that the bypass mass flow rate could be controlled sequentially from the start to the end of the condenser.

As presented in Fig. 4, the outer and inner diameters were 15.88 and 13.88 mm, respectively. *A*1-mm-thick aluminum tube was used. Trapezoidal grooves were processed on the inner wall, which supplied capillary pressure to circulate the working fluid. Each groove had a 2 mm height, 0.7 mm base length, and 0.93 mm tip length. Considering compatibility with the container material, acetone under 99% high purity was applied as the operating fluid. The entire length of the heat pipe was 750 mm, the lengths of the evaporator and the condenser were the same at 200 mm, and the remaining 350 mm was designed as an adiabatic section.

The bypass line had a 6.35 mm outer diameter and was composed of the same aluminum tube as the vessel of heat pipe. As presented in Fig. 3, the bypass tube was linked at the start of the evaporator and continued to the three liquid bypass ports installed in the condenser. As apparent from Figs. 2 and 3, the number of bypass ports installed in the condenser and their positions were important experimental variables that significantly affected the liquid-bypass mass flow rate.

The goal of this experimental work was to compare the thermal performance of the normal operation mode (NOM), in which all bypass valves were closed, and the bypass-line operating mode (BOM), in which the heat pipe was operated with the bypass tube. The thermal performance was examined for variations in the bypass valve ON/OFF settings. Note that if the working-fluid charging value is excessive, a liquid pool

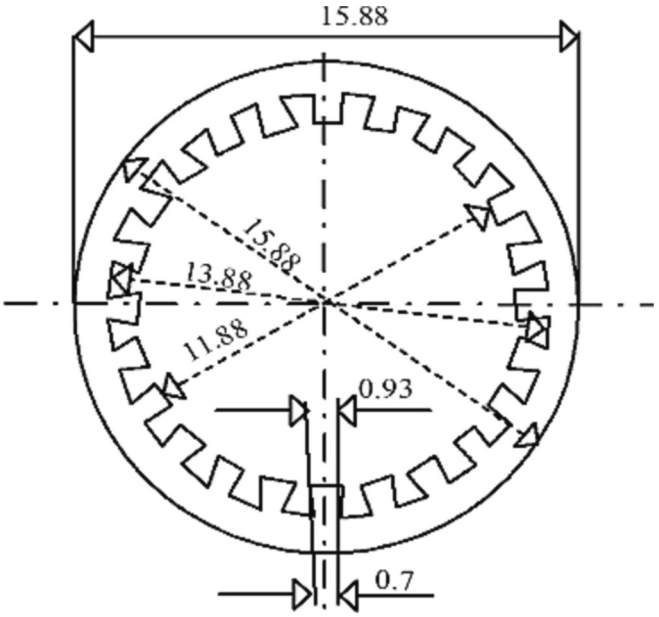

Fig. 4. Cross-sectional dimensions of grooved heat pipe.

forms within the container of the heat pipe, and the thermal performance decreases. However, if the charging value is too small, the value of Q_{in} that can be handled by the heat pipe may be reduced. Moreover, in this study, the optimal charging value under NOM from the heat pipe in Fig. 3(b) may have differed from that of the typical heat pipe presented in Fig. 3(a), because of the presence of the installed bypass ports. Therefore, a preliminary experiment was performed to compare the thermal resistance of a typical heat pipe and the newly designed heat pipe operating under NOM, with the charging value as an experimental variable. The working-fluid fill charge ratio of the heat pipe was determined under NOM on the basis of preliminary experimental work. The charging ratio of the working fluid, Φ, corresponded to 120% of the groove void volume, with 17.6 ml of working fluid being charged.

The thermal load was supplied to the evaporator by four cartridge-type electric resistance heaters with 1 kW capacities, which were

embedded in a heater block composed of aluminum material that surrounded the whole evaporator. The thermocouples employed in the experiment were K-type, with an AWG number of 30 and a wire diameter of 0.25 mm. We measured the surface wall temperature at seven major points of the heat pipe in the axial direction; Fig. 5 shows the thermocouple positions. Three thermocouples were bonded at equal intervals to sense the temperatures ($T_{evap.1}$, $T_{evap.2}$, and $T_{evap.3}$) on the outer wall of the evaporator, and similarly, three thermocouples were bonded at identical intervals to measure the temperatures ($T_{cond.1}$, $T_{cond.2}$, and $T_{cond.3}$) on the external wall of the condenser. The adiabatic temperature ($T_{adia.}$) was gauged by a thermocouple bonded to the center of the entire length of the heat pipe. To detect the liquid bypass flow, four thermocouples (T_{BL1}, T_{BL2}, T_{BL3}, and T_{BL4}) identical to those attached to the outer wall were bonded to the bypass line. They were adhered to the outlet of each bypass valve to detect the bypass flow passing through the valves. Probe-type thermocouples with 3 mm diameters were installed at the coolant inlet and outlet ($T_{cool.in}$ and $T_{cool.out}$, respectively) to measure the recovery heat released from the heat pipe condenser to the coolant. These thermocouples were calibrated within a 0.1 °C error in the range of 5–100 °C.

As shown in Fig. 5, the coolant was water, the temperature of which was controlled to a constant value by an isothermal bath. The isothermal bath had a maximum isothermal capacity of 1 kW at 3 °C. Throughout the experiment, the volume flow rate ($\dot{V}$) of the coolant was detected by a rotameter with an uncertainty of 4% of the maximum full scale (4 L/min) and was constantly controlled to 3 L/min. The temperature data obtained by the thermocouples were detected and collected at one second intervals by a data acquisition (DAQ) system. Further, Q_{in} was regulated to a constant value by a variable autotransformer (voltage regulator) and monitored by employing a power meter with an uncertainty of 0.5% of the full scale. The uncertainties for the instruments applied in the experiments on the heat pipe system are indexed in Table 1. These uncertainties were provided by a professional calibration company for the instrument. The uncertainty of the measuring device can be evaluated as described in [21]. The uncertainty of the experimental setup with N instruments can be expressed as follows by using the square root of the sum of the squares:

$$U_m = \sqrt{U_1^2 + U_2^2 + U_3^2 + \ldots + U_N^2}. \quad (1)$$

Table 1
Uncertainties of experimental instruments.

Instrument	Error	Uncertainty
Thermocouple (OMEGA, K-type, 30 AWG)	0.5 °C	0.00175
Thermal load monitor (ISM, HD - 301 M)	0.5%	0.005
Isothermal bath (Neslab, RTE - 111)	0.1 °C	0.0004
Data acquisition system (Fluke, NetDAQ2640A)	0.01%	0.0001
Flow meter (Dwyer, RMA - 2)	0.5 cc	0.04

When the uncertainty of each of the five instruments presented in Table 1 was calculated according to Eq. (1), the uncertainty of the experimental setup was evaluated to be 4%. All components applied to the heat pipe system were thoroughly cleaned with acetone inside the ultrasonic cleaner. The entire experimental process was conducted in a laboratory environment with constant room temperature control. The entire experimental set was well isolated by ceramic wool to hinder heat exchange with the external environment.

The thermal loss could be evaluated by the energy conservation between the thermal energy released to the coolant and the input thermal load, and the physical expression for the recovery heat (Q_{out}) is

$$Q_{out} = \left(\rho \dot{V} c\right)_{cool} (T_{cool.out} - T_{cool.in}), \quad (2)$$

where $T_{cool.in}$ and $T_{cool.out}$ are the inlet and outlet temperatures of the coolant, respectively. $\dot{V}$ is the volume flow rate of the coolant winding around the condenser. The entire heat pipe system was substantially insulated to minimize thermal correspond with the room, and the heat loss from the error of energy conservation between Q_{out} and Q_{in} was measured to be <10%.

The principal purpose of this work was to measure experimentally the variation in Q_{max} according to increases in the bypass flow rate. To this end, four flow-rate control valves were installed to the four bypass ports, as shown in Figs. 2 and 3. Three flow-rate control valves (BLFV #2–#4) were attached to the bypass ports at the start, middle, and end of the condenser. For the bypass line to be activated, the valve attached to the evaporator (BLFV #1) was opened, followed by the valves attached to the condenser, beginning with that attached to the start of the section (i.e., BLFV #2). Note that the bypass mass flow rate was increased by sequential opening of BLFV #2 to #4. When a valve at a given point of

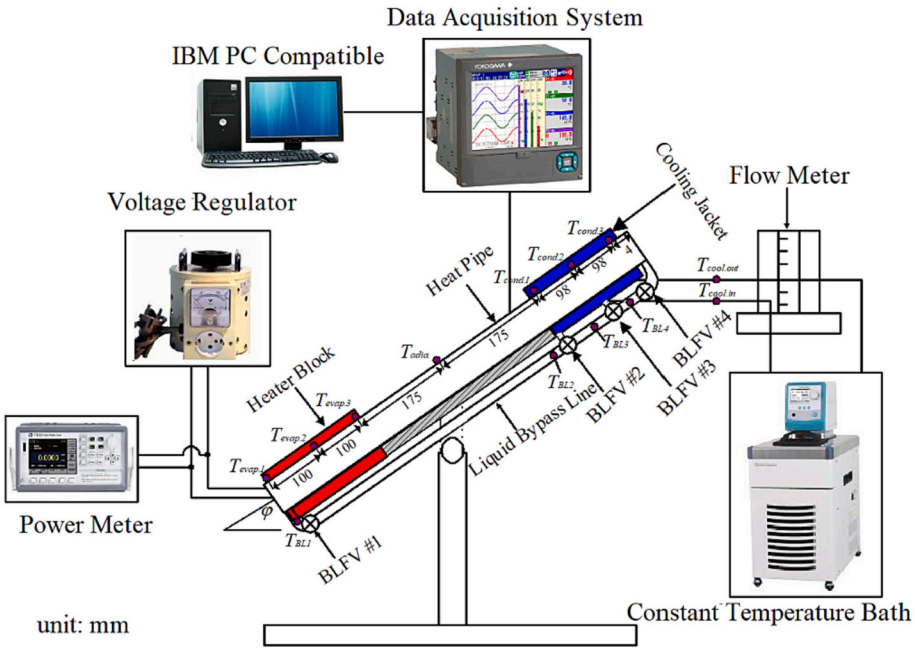

Fig. 5. Experimental setup of heat pipe system, including thermocouple locations.

the condenser was opened, the corresponding bypass port was activated. Table 2 lists the operating modes employed in this experiment. As noted above, NOM was the condition under which all valves in the bypass line were closed. BOM indicates a condition under which one or more valves were opened (classified into three modes). Therefore, four operating modes were employed in all experiments. As shown in Figs. 2, 3, and 5, BLFV #1 must be open for liquid bypass to be achieved normally. Normal liquid bypass by activation of BLFV #3 can be achieved by opening BLFV #2. In addition, normal liquid bypass by activation of BLFV #4 can be achieved by opening BLFV #2 and #4. Therefore, as shown in Fig. 2, no operation mode exists other than the working mode described in Table 2.

3. Results and discussion

3.1. Operation of the liquid bypass line

The maximum thermal load is determined by the geometric configuration of the heat pipe container, the working fluid, the characteristics of the capillary structure, and the operating environment. In previous studies [17,18], dryout limiting maximum heat transfer was found to be caused by insufficient liquid resupply from the condenser to the evaporator.

The mathematical models for the maximum thermal load developed so far have significant restrictions in that they are limited to well-defined boundary conditions or operating conditions. Research on the prediction of the maximum thermal load that can operate normally without experiencing the capillary limit was first conducted by Cotter [22] in 1965. Since then, several prediction models [23,24] for the maximum thermal load have been developed, but all of these models have a disadvantage in that they are expressed under a fully saturated evaporator wick structure. In the experiment of Shishido et al. [25], the vicinity of the capillary structure where the capillary limit was observed was not saturated by the working fluid, and the drying phenomenon was experimentally measured. In particular, a rigorous mathematical model for the dryout of a heat pipe operating under two-phase flow has not yet been found. The work on the development of analytical models faces considerable difficulties due to two-phase flow under the capillary environment with the counter flow between vapor and liquid. Therefore, dryout caused by the capillary limit is mainly observed through experiments. In experimental studies on dryout [17,18], liquid could be insufficiently supplied from the condenser to the evaporator due to the lack of capillary pressure under high thermal load. Under these conditions, dry phenomena were observed in the wick located at the beginning of the evaporator. According to these experiments, failure on the normal operation of the heat pipe is caused by the occurrence of a dry phenomenon on the wick structure located at the beginning of the evaporator.

On the other hand, an analytical model for the maximum thermal load that can be operated normally by capillary pressure was provided by Chi [26] in 1976. This model is the best known and most commonly applied in the design and manufacturing of heat pipes. The heat pipe with the bypass line in this study originated from physical consideration of the analytical model [26]. The derivation processes and physical meanings of the analytical model have been provided in various literatures [27] and were derived by the pressure balance between the pressure of the working fluid (vapor and liquid) and the capillary pressure. The physical expressions of the capillary limit for the heat transport factor are

$$Q_{cap.max} = \frac{(QL)_{cap.max}}{0.5L_{cond.} + L_{adia.} + 0.5L_{evap.}} \tag{3}$$

$$(QL)_{cap.max} = \int_0^{L_t} Q dz = \frac{\frac{2\sigma}{r_{cap.}} - \Delta P_g - \rho_l g L_t sin\varphi}{F_l + F_v} \tag{4}$$

where

$$F_v = \frac{2(f_v Re_v)\mu_v \dot{m}_v}{d_{h,v}^2 A_v \rho_v Q} \tag{5}$$

$$F_l = \frac{\mu_l \dot{m}_l}{K A_w \rho_l Q} \tag{6}$$

As shown in Eqs. (3) and (4), the maximum heat transfer rate ($Q_{cap.max}$) for which the effective capillary force can be maintained under normal operation of the heat pipe strongly depends on heat transfer factor ($(QL)_{cap.max}$). As shown in Eq. (4), F_v and F_l in Eqs. (5) and (6) must be reduced in order to increase $(QL)_{cap.max}$. As shown in Eqs. (5) and (6), except for the geometric dimensions of the heat pipe and the properties of the working fluid, F_l and F_v are strongly proportional to the mass flow rates ($\dot{m}_l$ and $\dot{m}_v$) of the liquid and vapor. The mass flow rates of the vapor and liquid inside the heat pipe are equal and can be determined by the input thermal load. Therefore, F_v and F_l can be reduced by reducing the mass flow rate of the liquid or vapor.

In general, a dry phenomenon occurs in the wick from the start of the evaporator due to the lack of liquid returning from the condenser to the evaporator under an input thermal load of $Q_{cap.max}$ or more. Considering the bypass of the condensed liquid to the beginning of the evaporator without going through the inner space of the heat pipe, the maximum thermal load can be expanded to some extent because more liquid supply to the start of the evaporator can be achieved. In addition, as shown in Eq. (4), a reduction in F_l can be achieved because the mass flow rate of the liquid returning through the wick to the evaporator is reduced by the bypassed liquid. Therefore, an acceleration effect for the working fluid can be obtained as the resistance due to friction is reduced in a flow having a counter flow of liquid and vapor. According to Eq. (5), the friction coefficient (F_v) of vapor can be reduced because an increase in the cross-sectional area (A_v) for the vapor space is induced by a decrease in the mass flow rate of the liquid in the inner space of the heat pipe. On the other hand, the shear stress over the liquid–vapor interface [28], τ_{lv} [$= \dot{m}_l(u_v - u_l)$], is directly proportional to the mass flow rate of the liquid, so the reduction of the interface resistance can be achieved most effectively by reducing the mass flow rate of the liquid.

Consequently, the installation of a device that enables the liquid to be bypassed in a typical heat pipe can provide more liquid to the evaporator. In addition, the acceleration effect of the working fluid can be achieved by reducing the flow resistance at the liquid–vapor interface. According to Eqs. (4)–(6), $Q_{cap.max}$ can be further increased by bypassing as much liquid mass flow as possible. Therefore, an experiment to improve the heat transfer performance of the heat pipe should be performed with respect to an increase in the mass flow rate of the bypassed liquid. The bypassed mass flow rate, $\dot{m}_{bl}$ [$= A_{bl}u_{bl}$] can be increased when the area (A_{bl}) of the condenser open to the bypass tube is increased.

Table 2
Operating modes.

Operating mode	BLFV #1	BLFV #2	BLFV #3	BLFV #4
	On/Off	On/Off	On/Off	On/Off
NOM	Off	Off	Off	Off
BOM I	On	On	Off	Off
BOM II	On	On	On	Off
BOM III	On	On	On	On

3.2. Effect of the bypass line on the maximum thermal load of a heat pipe

A sequence of tests was performed to measure the maximum thermal load (Q_{max}) according to the variation in the bypass flow rate. The coolant temperature was fixed to 3 °C, and the slope (φ) of the heat pipe and input thermal load (Q_{in}) were designated as the important experimental variables. The maximum φ value was set to 50° considering the

cooling capacity of the isothermal bath.

Fig. 6 shows the influence of the fill charge ratio (Φ) on the thermal performance under NOM according to Q_{in}, where Φ was increased from 80% to 140%. For all Q_{in}, the highest R_{th} value was measured when Φ was 140%. When Q_{in} was 50 and 100 W, the lowest R_{th} value was measured for Φ values of 100% and 110%, respectively. When Q_{in} was 150 and 200 W, the lowest R_{th} value was observed at Φ = 120%. According to Fig. 8, the optimal Φ value for the heat pipe with the bypass system was determined to be 120%.

As noted in Section 2, a preliminary experiment was performed to compare the heat transfer performance of a typical heat pipe (Fig. 3(a)) with that of the heat pipe with the bypass line under NOM. As apparent from Fig. 3, the NOM heat pipe was identical to the typical heat pipe if the four bypass ports installed to the evaporator and condenser were excluded. The index for comparing heat transfer performance of heat pipes is the thermal resistance, defined as follows:

$$R_{th} = \frac{\left(\overline{T}_{evap.} - \overline{T}_{cond.}\right)}{Q_{in}}, \tag{7}$$

where $\overline{T}_{evap.}$ and $\overline{T}_{cond.}$ are the average temperatures of the outer walls of the evaporator and condenser, respectively.

To evaluate the uncertainty of R_{th}, Ref. [29] was consulted; the results are presented in Fig. 7. A comparison of uncertainty in thermal resistance between a typical heat pipe and a heat pipe operated under NOM is presented in Fig. 7. The discrepancy between the uncertainties in the thermal resistance between the two heat pipes was calculated to be at most 3.6% (Q_{in}= 50 W) and <4% overall. The uncertainty of the thermal resistance measured in the operation of a typical heat pipe was generally <10%, and the maximum uncertainty was found to be 9.9% (Q_{in}= 100 W). The uncertainty of the thermal resistance measured in the heat pipe with NOM was generally evaluated to be <11%, and the maximum uncertainty was found to be 10.1% (Q_{in}= 100 W). Under input thermal loads of 50 and 100 W, the uncertainty of the typical heat pipe was calculated to be lower than that of the NOM heat pipe, but when the input thermal load exceeded 100 W, the uncertainty of the NOM heat pipe was calculated to be lower.

Fig. 8 compares the thermal resistance (R_{th}) results obtained for the typical and NOM heat pipes in the horizontal position. For the heat pipe in the horizontal position, R_{th} decreased as Q_{in} increased and was generally evaluated to be <10%. As shown in Fig. 8, the maximum R_{th} error was found to be 11% (Q_{in} = 50 W) and was generally <5% when Q_{in} = 50 W was excluded. The R_{th} of the typical heat pipe was lower under smaller thermal loads (50 and 100 W). However, R_{th} was lower for the modified heat pipe in the normal operation condition as

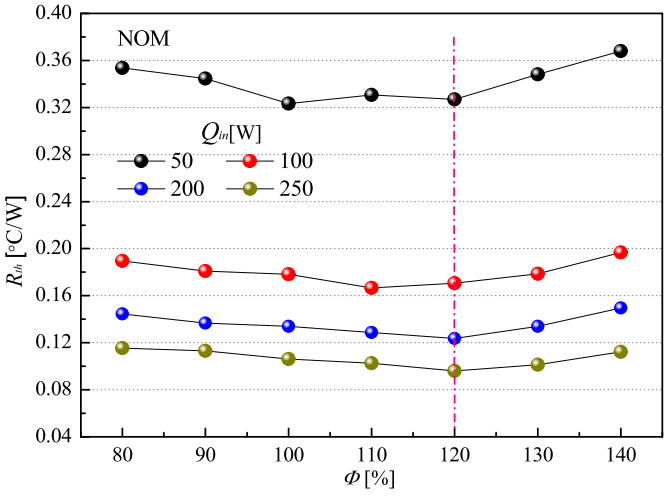

Fig. 6. R_{th} versus fill charge ratio for various input thermal loads with the heat pipe in the horizontal position.

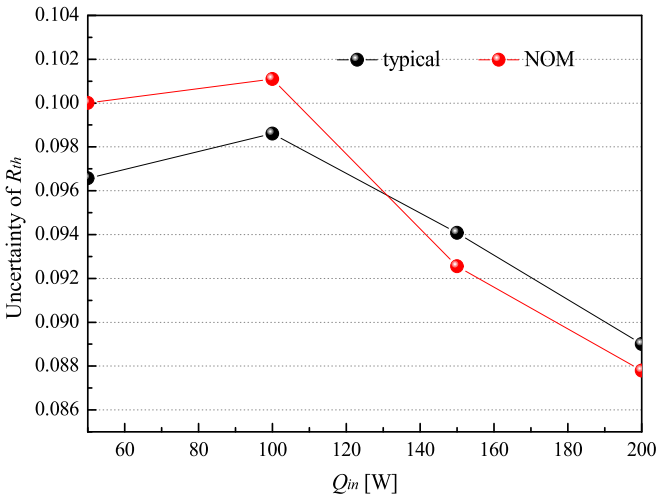

Fig. 7. Uncertainty of R_{th} for a heat pipe in the horizontal position.

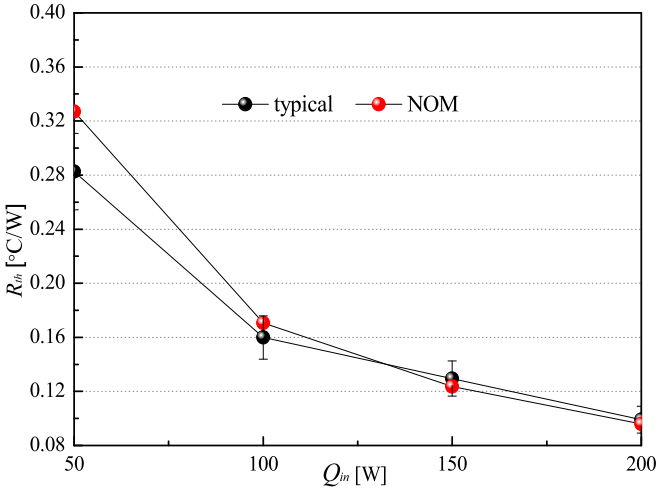

Fig. 8. Thermal resistance comparison for NOM condition and typical heat pipe in horizontal position.

the thermal load increased. In the case of the NOM heat pipe, it was estimated that the thermal resistance decreased slightly due to the increase in the volume of the heat pipe by the bypass port under high thermal load.

Fig. 9 shows the energy conservation between Q_{in} and the recovery heat released from the condenser to the coolant (i.e., Q_{out}) with $\varphi = 0°$. By considering the characteristic advantages of heat pipes that can normally operate without gravity assistance by capillary pressure, the standard for heat transfer performance of heat pipes can be reasonably defined in a horizontal position. As apparent from the figure, the thermal energy loss (Q_{loss}) increased with increasing Q_{in}. As the minimum and maximum Q_{loss} values were calculated to be 5.1% (at 100 W of the Q_{in}) and 7.9% (at 200 W of the Q_{in}), respectively, the overall error was <10%.

Figs. 10–12 show the Q_{max} values experimentally obtained for each operating mode (see Table 2) and for various φ values. The experiment was performed to determine Q_{max} and the minimum thermal load ($Q_{min.dryout}$) that caused dryout. First, for all operating modes, Q_{in} was increased in increments of 50 W from 50 W until dryout was observed; this approach was adopted to confirm the Q_{in} range that caused dryout. Next, as shown in Figs. 10–12, Q_{max} and $Q_{min.dryout}$ were measured with an error of 10 W, by reducing the Q_{in} range as much as possible.

Fig. 10(a)–(d) present the results obtained when Q_{in} was increased

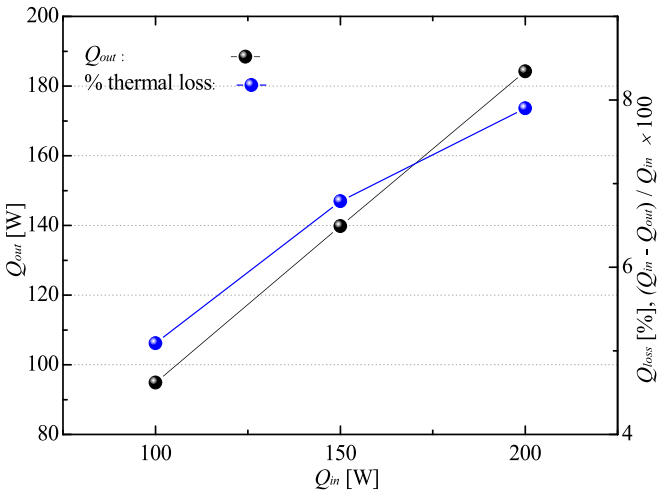

Fig. 9. Energy balance between Q_{in} and Q_{out} for heat pipe in horizontal position.

from 200 W to $Q_{min.dryout}$ for NOM and BOM I–III, respectively, with $\varphi = 0°$. As detailed in Table 2, the difference among BOM I, II, and III was the number of bypass ports activated in the condenser. For BOM I to BOM II and then BOM III, the bypass ports were sequentially activated from that located at the start of the condenser (BLFV #2). As apparent from Fig. 10, Q_{max} and $Q_{min.dryout}$ increased with the number of activated condenser bypass ports and, accordingly, the increased bypass flow rate through the bypass line. This outcome is attributed to the fact that the vapor and liquid pressure drops within the heat pipe reduced as the volume flow rate inside bypass tube increased, as explained in Section 1. In Fig. 10, overshooting was measured for the external wall temperature of the evaporator during startup, which was due to a delay in the arrival of the fluid bypassed from the condenser at the evaporator under the BOM, when the pipe was in the horizontal position. For this setup, Q_{max} and $Q_{min.dryout}$ were measured as 240 and 250 W under NOM, respectively, and as 260 and 270 W under BOM I, respectively, increasing by 20 W compared to the NOM case. When all three ports in the condenser were activated, Q_{max} and $Q_{min.dryout}$ were measured as 350 and 360 W, respectively, corresponding to increases of 110 W (up to 45.8%) over the NOM values. The percent improvement of the maximum thermal load was defined as a measure of BOM relative to NOM.

Fig. 11 shows the changes in T over time according to increases in Q_{in} for all operating modes presented in Table 2 and $\varphi = 10°$. As apparent from the figure, the overshoot problem was not measured for outer wall of the evaporator, because the bypass flow arrived at the evaporator quickly during startup of the heat pipe, unlike for the horizontal condition. Under NOM (Fig. 11(a)), the supplied Q_{in} values were 500, 520, 530, and 540 W, and Q_{max} and $Q_{min.dryout}$ were measured as 530 and 540 W, respectively. Under BOM I (Fig. 11(b)), Q_{in} values of 450, 500, 540, 550, 560, and 570 W were supplied, and Q_{max} and $Q_{min.dryout}$ were measured to be 560 and 570 W, respectively. Under BOM II (Fig. 11(c)), Q_{in} values of 500, 550, 580, 590, and 600 W were supplied, and Q_{max} and $Q_{min.dryout}$ were measured to be 590 and 600 W, respectively. For BOM III (Fig. 11(d)), for which all condenser bypass ports were activated, Q_{in}

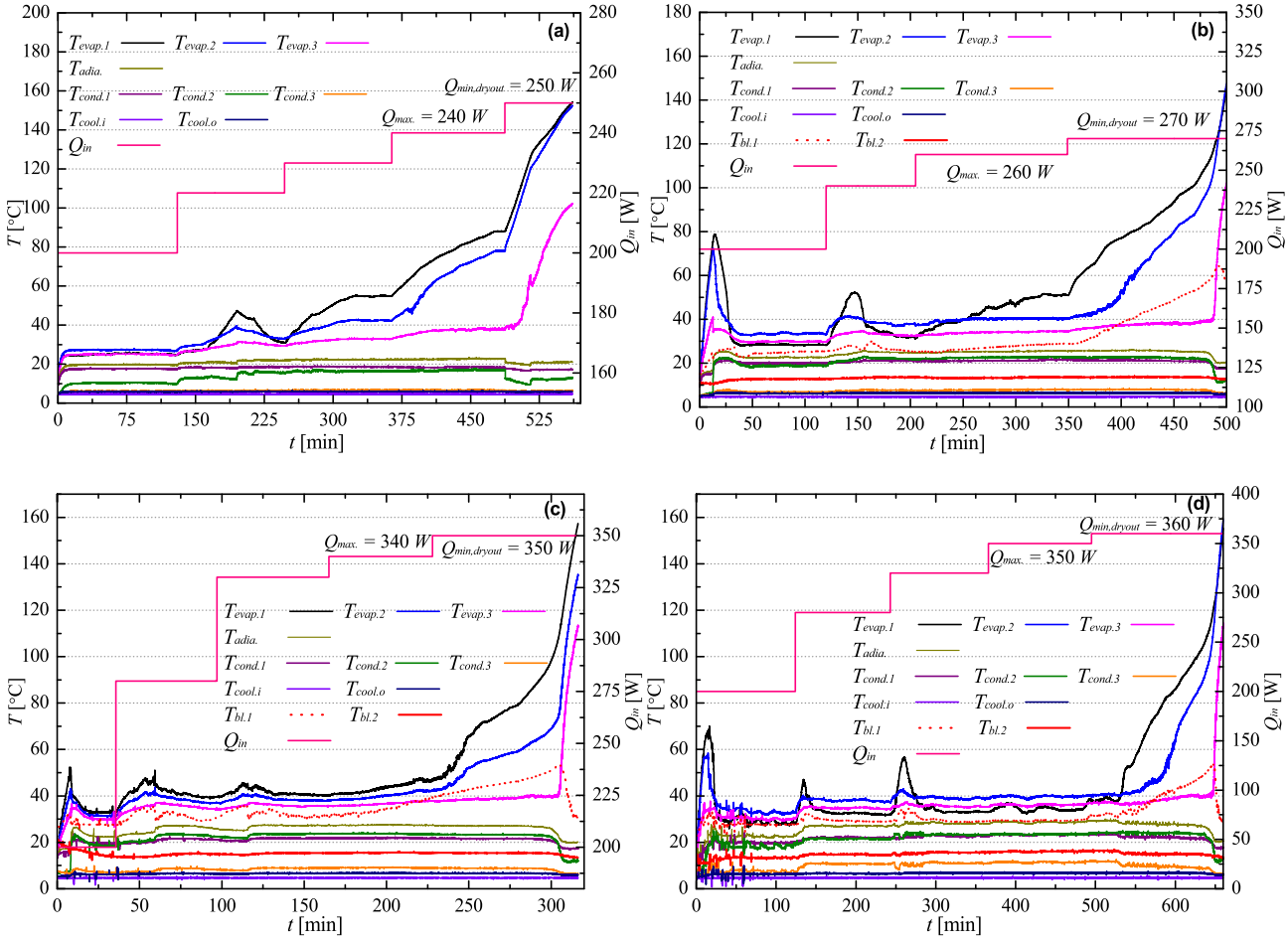

Fig. 10. Temperature history with increments of Q_{in} and maximum thermal load (Q_{max}) measurement for (a) NOM, (b) BOM I, (c) BOM II, and BOM III, with heat pipe in horizontal position.

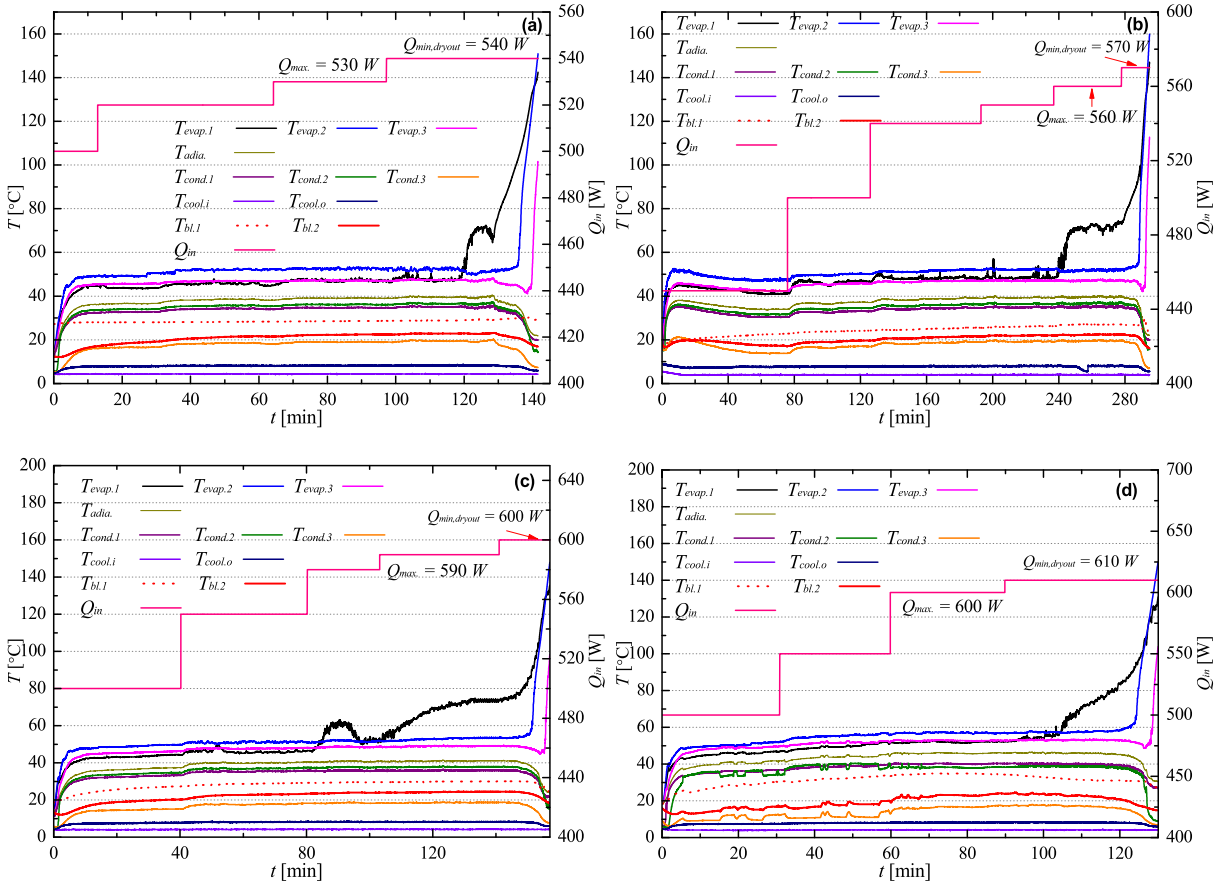

Fig. 11. Temperature history with increments of Q_{in} and Q_{max} measurement for (a) NOM, (b) BOM I, (c) BOM II, and BOM III, at a tilt angle (φ) of 10°.

values of 500, 550, 600, and 610 W were supplied, and Q_{max} and $Q_{min.dryout}$ were measured to be 600 and 610 W, respectively. For the heat pipe temperature, the thermal insulation temperature ($T_{adia.}$) is usually defined as the operating temperature. The $T_{adia.}$ values of 38, 36.6, 36.37, and 42.4 °C were measured for NOM, BOM I, BOM II, and BOM III, respectively. These values were generally lower under BOM compared to NOM, but that under BOM III was exceptionally high. The maximum evaporator wall temperature was measured at the middle of the section ($T_{evap.2}$), and similar values of 49.2, 50.3, 49.7, and 52.5 °C were obtained for NOM, BOM I, BOM II, and BOM III, respectively. As shown in Fig. 11, the Q_{max} and $Q_{min.dryout}$ values measured under BOM were up to 13.2% higher than those obtained under NOM.

Fig. 12 presents the temperature changes of each section of the heat pipe over time according to Q_{in}, under the four operating conditions presented in Table 2 and for $\varphi = 20°$. In the case of normal operation mode (Fig. 12(a)), Q_{in} values of 550, 600, 620, and 630 W were used. Dryout occurred after an experimental time of 280 min when $Q_{in} = 630$ W, as the T values of the thermocouples attached to the start and middle of the evaporator increased rapidly. Under NOM, Q_{max} and $Q_{min.dryout}$ were measured to be 620 and 630 W, respectively. As provided in Fig. 12 (b), the supplied Q_{in} ranged from 600 to 680 W under BOM I, and Q_{max} and $Q_{min.dryout}$ were measured to be 670 and 680 W, respectively, i.e., 50 W higher than the values obtained under NOM. The values of $T_{evap.1}$ and $T_{evap.2}$ began to increase when $Q_{in} = 680$ W was supplied at an experimental time of 141 min. Dryout occurred after an experimental time of 248 min, as T rapidly increased. Under BOM II, Q_{in} was 600, 650, 680, and 690 W. When $Q_{in} = 690$ W was supplied at an experimental time of 271 min, dryout occurred as the entire evaporator wall temperature rapidly increased. Under BOM II, Q_{max} and $Q_{min.dryout}$ were measured to be 680 and 690 W, respectively; these values were 60 W higher than those obtained for NOM. Under BOM III (Fig. 12(c)), the Q_{in} values supplied to the heat pipe were 650, 690, and 700 W. For the 700 W case, the experiment was stopped at 232 min, because the evaporator wall temperature increased to 150 °C. Q_{max} and $Q_{min.dryout}$ were measured to be 690 and 700 W under BOM III, respectively; these values were 70 W higher that those measured for NOM. As shown in Fig. 12, at $\varphi = 20°$, Q_{max} increased by 50, 60, and 70 W as the number of bypass ports activated in the condenser increased. Q_{max} for BOM I, BOM II, and BOM III increased by 8.1%, 9.7%, and 11.3%, respectively, compared to the NOM case.

Experiments on the ON/OFF operation of the valves during operation were conducted to investigate the effect of the bypass line on the start-up and steady-state performance of the heat pipe. As the area of the bypass port in the condenser increased as shown in Figs. 10–12, Q_{max} of the heat pipe increased. The highest Q_{max} value was measured under BOM III operation. The principle that the bypass mode contributes to the maximum heat transfer performance can be described to some extent by analyzing the trend of the temperature distribution in the axial direction of the heat pipe through the mutual conversion operation between the NOM and BOM during the operation of the heat pipe.

Fig. 13 shows the temperature trends of the main points according to increasing Q_{in} under the operating conditions detailed in Table 2, for $\varphi = 50°$. As shown in Fig. 13(a), the Q_{in} values were 700, 740, and 750 W for the NOM case. When $Q_{in} = 750$ W was supplied at an experimental time of 66 min, dryout was observed, as the T values measured at the start and middle of the evaporator rapidly increased. Under NOM, Q_{max} and $Q_{min.dryout}$ were measured to be 740 and 750 W, respectively. In the state of BOM I (Fig. 13(b)), the Q_{in}values were 700, 750, 810, and 820 W. $Q_{in} = 820$ W was supplied at an experimental time of 85 min. Subsequently, the evaporator outer wall temperatures began to increase; they rapidly increased from approximately 171 min, causing dryout. As shown in Fig. 13(b), Q_{max} and $Q_{min.dryout}$ were measured to be 810 and

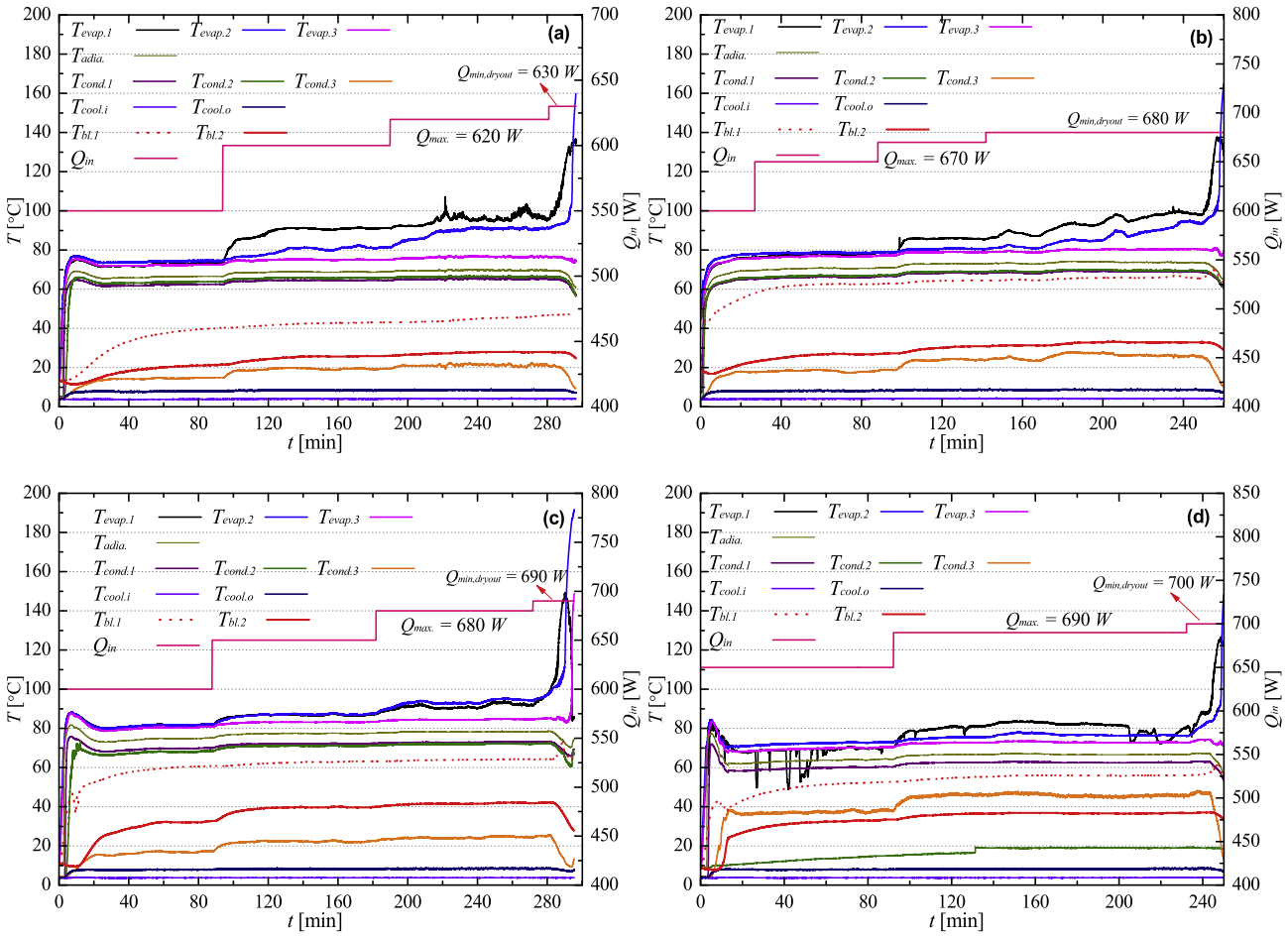

Fig. 12. Temperature history with increments of Q_{in} and Q_{max} measurement for (a) NOM, (b) BOM I, (c) BOM II, and BOM III, at $\varphi = 20°$.

820 W for BOM I and $\varphi = 50°$, respectively; these values were 70 W higher than those measured for NOM. Under BOM II (Fig. 13(c)), the Q_{in} values were 800, 880, and 890 W. Here, Q_{in} = 890 W was supplied at approximately 135 min, and dryout was observed at approximately 143 min, because of a rapid increase in the evaporator wall temperature. In this case, Q_{max} and $Q_{min.dryout}$ were measured to be 880 and 890 W, respectively, being 140 W higher than the values obtained for NOM. In the case of BOM III (Fig. 13(d)), Q_{in} values of 800, 850, 900, 940, and 950 W were sequentially supplied. Q_{in} = 950 W was supplied at approximately 128 min, and dryout was observed in approximately 3 min, with a rapid increase in the evaporator wall temperatures. As provided in Fig. 13(d), Q_{max} and $Q_{min.dryout}$ were measured to be 940 and 950 W for BOM III and $\varphi = 50°$, respectively; these values were 200 W higher than those obtained for NOM. As presented in Fig. 13, when the bypass operation modes (BOMs) were employed to the heat pipe at φ = 50°, Q_{max} increased by up to 25.3% compared to that for NOM.

As mentioned in Section 3.1, Q_{max} of the heat pipe increases as more condensed liquid is supplied to the evaporator, so the minimum thermal load that causes dryout can be increased. In Figs. 10–13, Q_{max} increased by up to 200 W (BOM III at $\varphi = 50°$) as the number of activated bypass ports installed in the condenser increased. As the number of bypass ports increases, an increase in Q_{max} can be estimated with an increase in the mass flow rate bypassed to the start of the evaporator. T_{BL1} increased with the increase in the area of the bypass port due to the increase in the wall temperature of the condenser due to the acceleration of the working fluid. As shown in Fig. 14, the steady-state value of T_{BL1} for NOM, BOM I, BOM II and BOM III at the horizontal with an input thermal load of 200 W was measured to be 29.6, 25.8, 27.4, and 28.2 °C, respectively. In the case of NOM, the highest T_{BL1} value was measured due to heat transfer by thermal conduction from the evaporator wall to the bypass tube located at the start of the evaporator. A lower T_{BL1} was obtained compared to the NOM due to the flow of the condensed liquid into the bypass tube under the BOM. Among the BOM operation modes, T_{BL1} of BOM III was measured to be the highest.

Fig. 15 shows Q_{max} according to the orientation angle φ under each operating condition. Clearly, Q_{max} increased as number of activated bypass ports installed in the condenser increased. In the case of BOM III, for which all bypass ports in the condenser were activated, Q_{max} increased by 10.3% ($\varphi = 15°$) to 45.8% ($\varphi = 0°$) compared to the values for NOM. Q_{max} increased the most significantly when the heat pipe had $\varphi = 0°$ because, at that angle, the portion of the bypassed flow rate for the entire liquid increased. This change occurred because the liquid remained in the condenser for a longer period of time, compared to the time periods for other φ values. In addition, Q_{max} was measured to be significantly higher for $\varphi = 50°$ than for the other φ values (exceeding 0°). No experiment was performed for $\varphi > 50°$ because of the limited capacity of the isothermal bath. Additional experiments at higher φ should be conducted in the future.

4. Conclusions

A capillary limit usually exists due to insufficient liquid resupply to n evaporator under high thermal loads. Insufficient liquid return to the evaporator causes a drying problem for the wick structure located at the beginning of the evaporator. In order to increase the maximum thermal load that can operate normally without dryout, more condensate liquid must be supplied at the beginning of the evaporator. In this study, a liquid bypass tube was connected between the condenser and

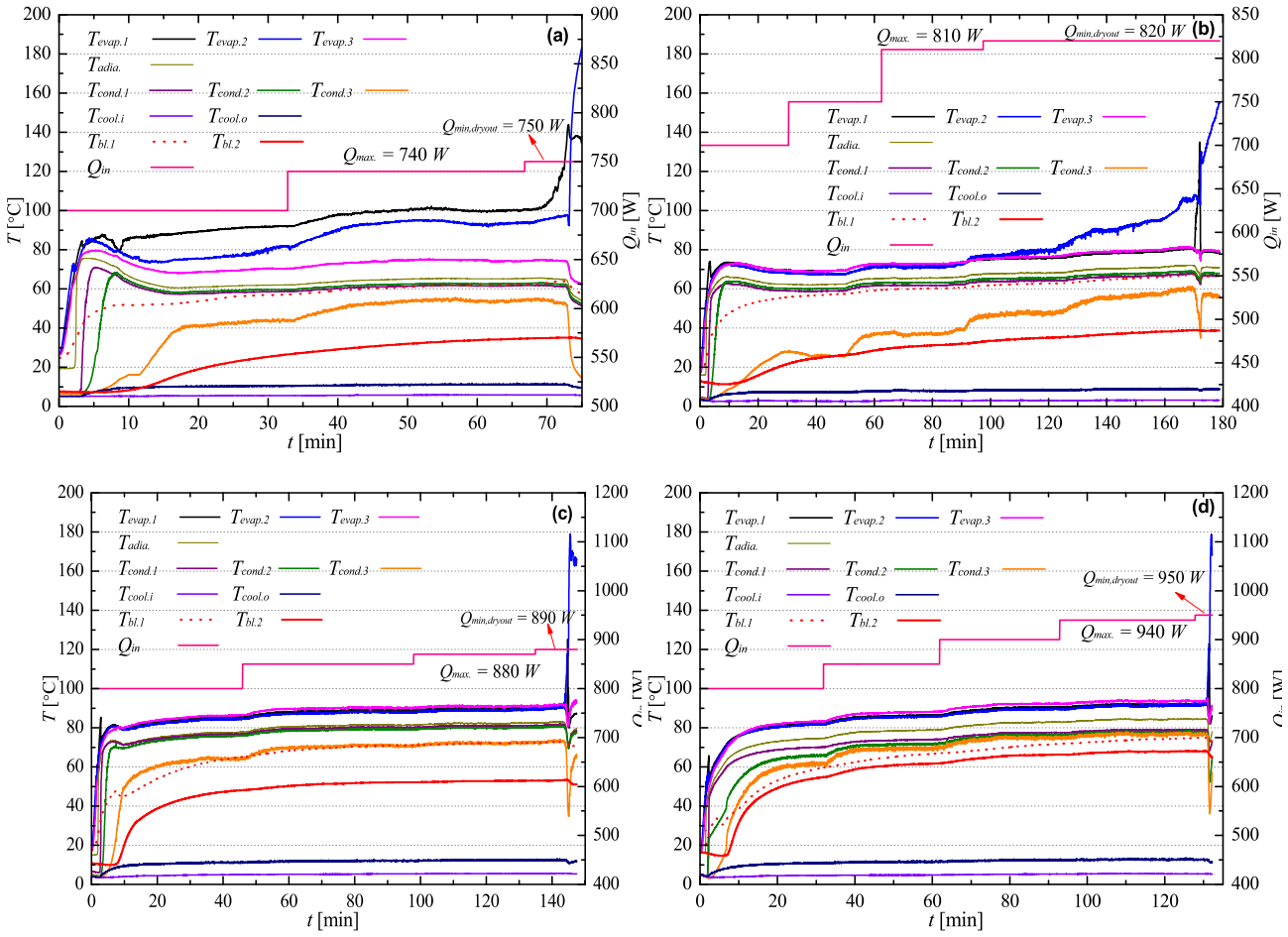

Fig. 13. Temperature history with increments of Q_{in} and Q_{max} measurement for (a) NOM, (b) BOM I, (c) BOM II, and BOM III, at $\varphi = 50°$.

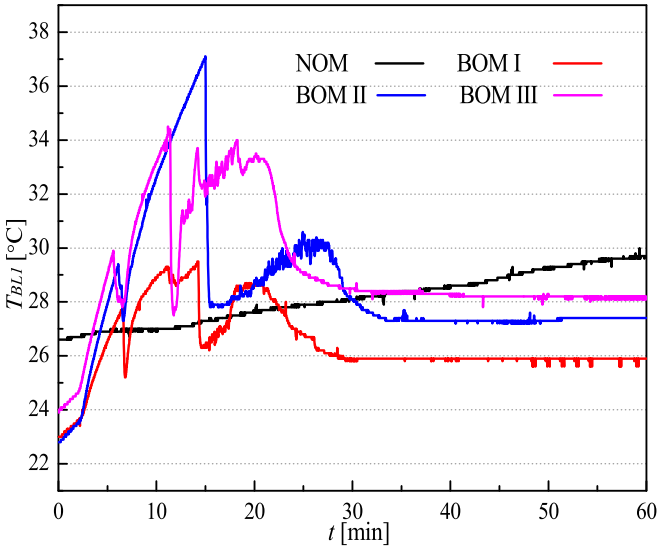

Fig. 14. Transient temperature histories for NOM, BOM I, BOM II, and BOM III at $\varphi = 0°$ and $Q_{in} = 200$ W.

evaporator of a typical heat pipe to enable the heat pipe to have an increased maximum thermal load. In particular, three liquid ports were attached to the condenser to investigate the changes in the maximum thermal load according to changes in the mass flow rate of the bypassed liquid. We assumed that the bypass flow increased with an increase in the number of activated ports. The maximum thermal loads for φ = 0°, 10°, 20°, 30°, 40°, and 50° were obtained within an error of 10 W. Through this experimental work, the following conclusions were obtained.

(1) The maximum thermal load that can operate normally without dryout was measured to be the highest in BOM III at all slopes, and the maximum thermal load increased with an increase in the number of bypass ports. As the condenser area open to the bypass tube is proportional to the bypassed mass flow rate, the maximum thermal load increases with the increase in the bypassed mass flow rate.
(2) When BOM III was applied at φ = 0° and 50°, the maximum thermal load increased to 45.8% and 25.3%, respectively.
(3) The overall temperature of the evaporator was lowered, and the temperature of the condensation was higher under the BOM. Thus, the isothermal performance of the heat pipe is improved. In particular, the significant increase in temperature at the end of the condenser was assumed to be due to some acceleration of the working fluid by the liquid bypass.
(4) Under the BOM, as the number of bypass ports increased, the wall temperature of the condenser increased, which increased the temperature of the bypass tube located at the beginning of the evaporator.

According to the experimental results of this study, the larger the area of the evaporator opened to the bypass port, the more liquid could be supplied to the evaporator. This characteristic enabled an increase in the maximum thermal load to be achieved. Therefore, in order to

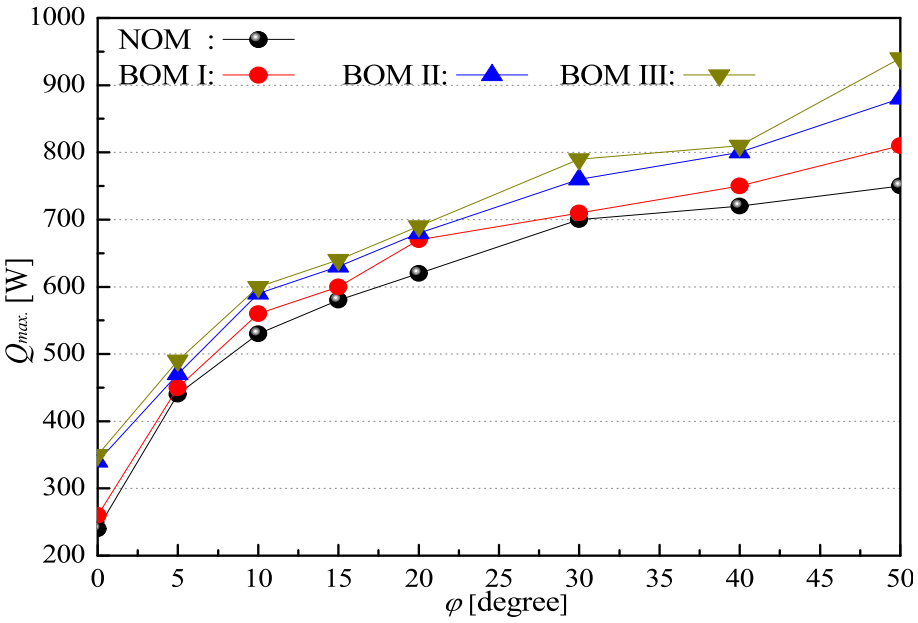

Fig. 15. Q_{max} of the heat pipe under NOM and BOM conditions versus φ.

maximize the heat transfer performance of the heat pipe by the liquid bypass, the area of the condenser opened to the bypass tube should be designed to be as large as possible.

Author contribution form

All authors must check the relevant terms to indicate their contributions. To know more about the CReDiT Author Statement and definitions of each term mentioned in the below form, please visit https://www.elsevier.com/authors/policies-and-guidelines/credit-author-statement

Term	Eui Guk Jung	Cheong Hoon Kwon	Gee Chan Jin	Jun Hyung Kim	Bo Gyu Im	Ji Hoon Jeong
Conceptualization	√	√				
Methodology / Study design	√	√				
Software						
Validation		√	√	√	√	√
Formal analysis	√					
Investigation	√	√				
Resources		√				
Data curation		√	√	√	√	√
Writing – original draft	√					
Writing – review and editing	√	√				
Visualization						
Supervision	√					
Project administration	√					
Funding acquisition	√	√				

#Use author initials to declare the contributions to the manuscript.
*Use tick mark (√) to indicate contribution, a cross (X) to indicate no contribution and NA where not applicable.

Declaration of Competing Interest

None.

Data availability

No data was used for the research described in the article.

Acknowledgement

This research was supported by a National Research Foundation of Korea (NRF) grant (No. NRF-2018R1D1A1B07040929, No. NRF2022R1F1A1066459 and No. NRF-2022R1A2C1009690) funded by the Korean Government (MSIT). Also, this work was supported by University Innovation Support Project through the National Research Foundation of Korea funded by the Ministry of Education.

References

[1] S. Abbas, Z. Ramadan, C.H. Park, Thermal performance analysis of compact-type simulative battery module with paraffin as phase-change material and flat plate heat pipe, Int. J. Heat Mass Transf. 173 (2021), 121269.
[2] S. Lei, Y. Shi, G. Chen, Heat pipe based spray-cooling thermal management system for lithium-ion battery: experimental study and optimization, Int. J. Heat Mass Transf. 163 (2020), 120494.
[3] H. Behi, D. Karimi, M. Behi, M. Ghanbarpour, J. Jaguem, M.A. Sokkeh, F. H. Gandoman, M. Berecibar, J. Mierlo, A new concept of thermal management system in Li-ion battery using air cooling and heat pipe for electric vehicles, Int. J. Heat Mass Transf. 174 (2020), 115280.
[4] M. Bernagozzi, A. Georgoulas, N. Miché, M. Marengo, Heat pipes in battery thermal management systems for electric vehicles: a critical review, Appl. Therm. Eng. 219 (2023), 119495.
[5] A. Faghri, Heat Pipe Science and Technology, Taylor & Francis, Washington, 1995, pp. 2–622.
[6] A. Brautsch, P.A. Kew, Examination and visualization of heat transfer processes during evaporation in capillary porous structures, Appl. Therm. Eng. 22 (2012) 815–824.
[7] R. Kempers, D. Ewing, C.Y. Ching, Effect of number of mesh layers and fluid loading on the performance of screen mesh wicked heat pipes, Appl. Therm. Eng. 26 (2006) 589–595.
[8] S.C. Wong, J.H. Liou, C.W. Chang, Evaporation resistance measurement with visualization for sintered copper-powder evaporator in operating flat-plate heat pipes, Int. J. Heat Mass Transf. 53 (2010) 3792–3798.
[9] R. Revellin, R. Rulliere, F. Lefèvre, J. Bonjour, Experimental validation of an analytical model for predicting the thermal and hydrodynamic capabilities of flat micro heat pipes, Appl. Therm. Eng. 29 (2009) 1114–1122.
[10] F. Lefèvre, M. Lallemand, Coupled thermal and hydrodynamic models of flat micro heat pipes for the cooling of multiple electronic components, Int. J. Heat Mass Transf. 49 (2006) 1375–1383.
[11] S.C. Wong, W.S. Liao, Visualization experiments on flat-plate heat pipes with composite mesh-groove wick at different tilt angles, Int. J. Heat Mass Transf. 123 (2018) 839–847.
[12] S. Lips, F. Lefèvre, J. Bonjour, Combined effects of the filling ratio and the vapor space thickness on the performance of a flat plate heat pipe, Int. J. Heat Mass Transf. 53 (2010) 694–702.
[13] S.C. Wong, Y.C. Lin, J.H. Liou, Visualization and evaporator resistance measurement in heat pipes charged with water, methanol or acetone, Int. J. Therm. Sci. 52 (2012) 154–160.

[14] A. Cecere, D.D. Cristofaro, R. Savino, G. Boveri, M. Raimondo, F. Veronesi, F. Oukara, R. Rioboo, Visualization of liquid distribution and dry-out in a single-channel heat pipes with different wettability, Exp. Thermal Fluid Sci. 96 (2018) 234–242.
[15] K.E. Pruzan, K.E. Torrance, C.T. Avedisian, Two-phase flow and dryout in a screen wick saturated with a fluid mixture, Int. J. Heat Mass Transf. 33 (1990) 673–681.
[16] Y.F. Maydanik, Loop heat pipes, Appl. Therm. Eng. 25 (2005) 635–657.
[17] E.G. Jung, J.H. Boo, Enhancement of the maximum heat transfer rate of the heat pipe through the bypass line, Appl. Therm. Eng. 198 (2021), 117461.
[18] Y.M. Baek, E.G. Jung, Experimental study on start-up and steady-state heat transfer performance of heat pipe with liquid bypass line for accelerating working fluid, Case Stud. Therm. Eng. 29 (2022), 101708.
[19] K. Baraya, J.A. Weibel, S.V. Garimella, Experimental demonstration of heat pipe operation beyond the capillary limit during brief transient heat loads, in: 18th IEEE ITHERM Conference, 2019, pp. 649–655.
[20] Q. Cai, Y.C. Chen, Investigations of biporous wick structure dryout, J. Heat Transf. 134 (2012), 021503.
[21] The American Society of Mechanical Engineers, Test uncertainty, ASME PTC 19 (2005) 1.
[22] T.P. Cotter, Theory of Heat Pipes, Report LA-3246-MS, Los Alamos Scientific Lab, Los Alamos, New Mexico, 1965.
[23] C.L. Williams, G.T. Colwell, Heat pipe model accounting for variable evaporator and condenser lengths, AIAA J. 12 (1974) 1261.
[24] K.R. Chun, Evaporation from a semi-infinite region with a nonvolatile solute, J. Heat Transf. 94 (1972) 238–240.
[25] I. Shishido, I. Oishi, S. Ohtani, Capillary limit in heat pipes, J. Chem. Eng. Japan 17 (1982) 179–185.
[26] S.W. Chi, Heat Pipe Theory and Practice, Mc Graw Hill, New York, 1976, pp. 33–95.
[27] B. Zohuri, Heat Pipe Design and Technology: Modern Applications for Practical Thermal Management, Springer, 2016, pp. 43–162.
[28] P.H. Oosthuizen, D. Naylor, Convective Heat Transfer Analysis, Second ed., McGraw-Hill, 1999, pp. 555–599.
[29] J.P. Holman, Experimental Methods for Engineers, McGraw-Hill, 1996.